Unique Characteristics of Imbalanced Torque Force of a Partial Admission Turbine for 50% Partiality

Kazuyuki Yada[1], Satoshi Kawasaki[2] and Masaharu Uchiumi[3]
Japan Aerospace Exploration Agency, Kakuda, Miyagi, 981-1525, JAPAN

and

Hiromasa Kato[4] and Ken-ichi Funazaki[5]
Iwate University, Morioka, Iwate, 020-8551,JAPAN

This paper describes a theoretical model of an imbalanced torque force, called the Thomas/Alford force, of a partial admission turbine for a rocket turbopump. The imbalanced torque force is a destabilizing force of the rotor, which may cause shaft vibration. A theoretical model is developed and some segment patterns for 50% partiality are tested. In this case, the 2/4 admission case, the motion of the Thomas/Alford force is unlike other typical admission patterns. The reason for this is investigated and it revealed by the mathematical method.

Nomenclature

a_i	=	Blockage function
C_0	=	Isentropic velocity
C_r	=	Initial tip clearance
F	=	Total tangential force
F_x	=	X -direction component of the tangential force increment
F_y	=	Y -direction component of the tangential force increment
F_P	=	Total excitation force
F_t	=	Tangential direction of total excitation force
F_n	=	Radial direction of total excitation force
F_{Tx}	=	X-direction excitation force
F_{Ty}	=	Y-direction excitation force
f	=	Tangential force increment
f_0	=	Mean tangential force increment
g_t, g_n	=	General trigonometric functions
H	=	Blade height
i	=	Phase index with tangential direction
K_{xx}	=	Direct stiffness coefficient
K_{xy}	=	Cross-coupled stiffness coefficient
U	=	Tip speed
β	=	Change in thermodynamic efficiency per unit change in clearance (Thomas coefficient)
δ	=	Actual tip clearance
ε	=	Amplitude of whirl
φ	=	Phase of a rotor
η_u	=	Loss caused by the change of efficiency of the blade

---

[1] Associate Senior Researcher, Research Unit IV, JAXA, Kakuda, Miyagi, 981-1525.
[2] Associate Senior Researcher, Research Unit IV, JAXA, Kakuda, Miyagi, 981-1525.
[3] Manager, Research Unit IV, JAXA, Kakuda, Miyagi, 981-1525.
[4] Assistant Professor, Department of Mechanical Engineering, Iwate University, Iwate, 020-8551.
[5] Professor, Department Mechanical Engineering, Iwate University, Iwate, 020-8551.

θ	=	Instant angle of a rotor
ψ	=	Phase of excitation force between total excitation force direction and radial direction

Subscript

F	:	Full admission
P	:	Partial admission

I. Introduction

The Thomas/Alford force is one of the important forces with regard to unsteady radial shaft vibration and may cause destruction of a rocket turbopump. This force is based on torque imbalance from tip clearance variation of a turbine wheel caused by the whirling motion of the rotor system of the turbopump. A small tip gap of a turbine blade results in high efficiency because of small leakage loss and indicates the existence of a large tangential force above the mean tangential force. On the other hand, a large tip gap causes opposite tendencies. The schematic shown in Fig.1 describes this situation. This force was firstly reported by Thomas[1] and Alford[2] independently. They defined the force of general full admission turbines theoretically. By introducing an empirical coefficient, i.e., a Thomas coefficient, the theoretical model can describe actual destabilizing force of turbines.

Motoi et al.[3] tried to derive the Thomas/Alford force by CFD for the case of the full admission turbine of the LE-7A Japanese rocket engine. Hendricks et al.[4] reviewed rotordynamic issues of turbomachines, including the study of Motoi et al.[3]. Kanki and Tanitsuji[5] firstly developed a theoretical Thomas/Alford force model of a partial admission steam turbine[6,7]. However, there are few cases in which those theories have been applied to turbines for rocket turbopumps.

An upper stage rocket engine usually has a narrow flow passage area, and the blade height of the full admission turbine is sometimes too short to gain sufficient efficiency. The key point of the upper stage rocket engine is efficiency. The flow rate in the turbine is usually small. A sufficient power supply even with a small flow rate is needed for high turbine efficiency. An alternative approach is an adoption of a partial admission turbine. The partial admission turbine of the rocket turbopump is utilized for a typical upper stage rocket engine in order to increase aerodynamic efficiency[8]. Nevertheless, it is still unclear how the partial admission turbine performs in terms of aerodynamics, structure and vibration.

In this paper, vibrational characteristics of a partial admission turbine for the rocket trubopump is studied in consideration of the methodology of the Thomas/Alford force. A theoretical Thomas/Alford force model based on Kanki et al.[5] is applied to the partial admission turbine. Typical partial admission patterns are investigated theoretically and the most effective pattern is determined in this study along with its mathematical reasoning. Undesired vibrational characteristics of the partial admission patterns are also revealed.

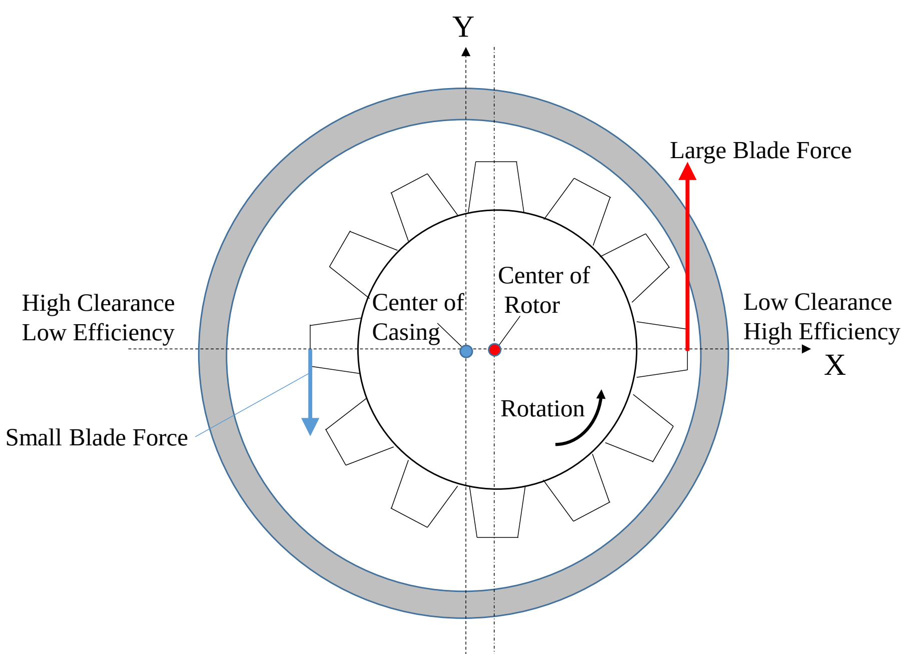

Figure 1. The schematic of the Thomas/Alford force.

II. Theoretical model of Thomas/Alford force

A. Thomas/Alford force of the full admission turbine

Alford[2] developed a theoretical model of the Thomas/Alford force of general turbines. Local torque per radian is proportional to the ratio of eccentricity to blade height or bucket height. Thus, the Thomas/Alford force is expressed by eq. (1).

$$K_{xy} = \frac{F\beta}{2H} \tag{1}$$

Kanki et al.[5] defined the Thomas/Alford force expressed by eqs. (2) and (3). φ is the phase of a rotor and is an integrand around the rotor shown by Fig. 2. The loss η_u is defined following ref. 8,

$$F_{TFx} = -\frac{F}{2\pi}\int_0^{2\pi}\left\{\eta_u - \frac{\beta}{H}\left(C_r - \varepsilon\cos(\theta-\varphi)\right)\right\}\sin\varphi d\varphi \tag{2}$$

$$F_{TFy} = -\frac{F}{2\pi}\int_0^{2\pi}\left\{\eta_u - \frac{\beta}{H}\left(C_r - \varepsilon\cos(\theta-\varphi)\right)\right\}\cos\varphi d\varphi \tag{3}$$

where, the coordinate system is defined in Fig. 2. A whirl orbit is assumed to be a circle expressed by eq. (4).

$$\delta = C_r - \varepsilon\cos(\theta-\varphi) \tag{4}$$

Equations (2) and (3) are based on a coordinate system at rest. By rewriting Eqs. (2) and (3) in the rotating reference frame followed by some mathematical manipulations, the following expressions are obtained.

$$\begin{aligned} F_{TFx} &= -\frac{F}{2\pi}\int_0^{2\pi}\left\{\eta_u - \frac{\beta}{H}\left(C_r - \varepsilon\cos(\theta-\varphi)\right)\right\}\sin(\varphi-\theta)d(\varphi-\theta) \\ &= \left[\frac{F}{2\pi}\left(\eta_u - \frac{\beta}{H}C_r\right)\cos(\theta-\varphi) - \frac{F}{2\pi}\frac{\beta}{H}\varepsilon\sin^2(\theta-\varphi)\right]_0^{2\pi} \\ &= 0 \end{aligned} \tag{5}$$

$$\begin{aligned} F_{TFy} &= -\frac{F}{2\pi}\int_0^{2\pi}\left\{\eta_u - \frac{\beta}{H}\left(C_r - \varepsilon\cos(\theta-\varphi)\right)\right\}\cos(\varphi-\theta)d(\varphi-\theta) \\ &= \left[\frac{F}{2\pi}\left(\eta_u - \frac{\beta}{H}C_r\right)\sin(\theta-\varphi) + \frac{F}{2\pi}\frac{\beta}{H}\varepsilon\left\{\frac{\sin(\theta-\varphi)\cos(\theta-\varphi)}{2} + \frac{\theta-\varphi}{2}\right\}\right]_0^{2\pi} \\ &= \frac{F\beta}{2H}\varepsilon \end{aligned} \tag{6}$$

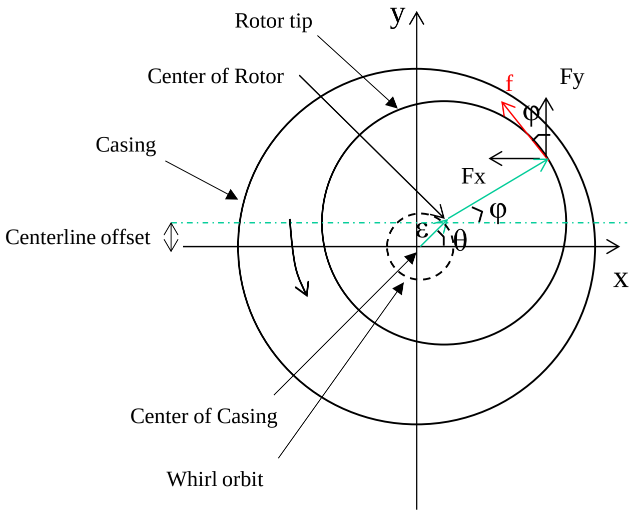

Figure 2. Coordinate of stage excitation force analysis.

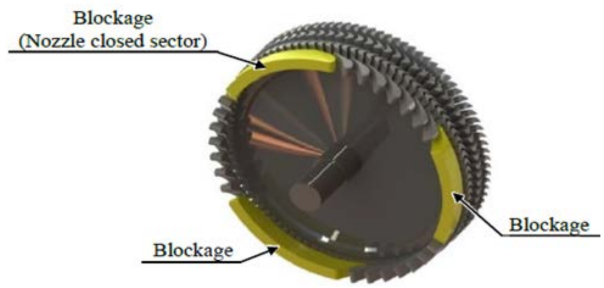

Figure 3. Schematic of the design of the partial admission turbine.

B. Thomas/Alford force of the partial admission turbine

The partial admission turbine is a turbine in which a part of the first nozzles is enveloped by plates, i.e. blockage, in order to increase the flow rate and height of blades. A schematic design of the partial admission turbine is shown in Fig. 3. This means higher turbine efficiency is obtained by the higher isentropic velocity ratio U/C_0. However, because of the existence of the blockage, the prediction of the Thomas/Alford force is more complicated and the prediction by CFD is much more difficult than that of the full admission turbine.

Kanki et al.[5] developed a theoretical model for the partial admission turbine. In the present study, the Thomas/Alford force of the partial admission turbine is developed based on the model of Kanki et al.[5] and is described in this section.

Regarding blade force per radian is assumed that the force variation is proportional to a ratio of δ/H expressed by eq. (7). The definition is the same as that of the full admission turbine. The main difference of the force between these turbines is that the force acts only on the open sector of the first nozzles in the partial adimission turbine. In other words, the force is zero in the closed sector (blockage). In the current theoretical model, the tangential direction is sub-divided by 1 deg to facilitate control of the blockage area, and following a_i is introduced. The Thomas/Alford force of the partial admission turbine is expressed by eqs. (8) and (9). Here, the loss such as η_u is set at unity since it is canceled by the force at ε =0 expressed later.

$$f = f_0\left\{1-\frac{\delta}{H}\beta\right\} = \frac{F}{2\pi R}\left\{1-\frac{\delta}{H}\beta\right\} \tag{7}$$

$$F_{TPx} = -\frac{180F_s}{\pi}\sum_{i=1}^{360}\left[a_i\int_{(i-1)\pi/180}^{i\pi/180}\left\{1-\frac{\beta}{H}\left(C_r-\varepsilon\cos(\theta-\varphi)\right)\right\}\sin\varphi d\varphi\right] \tag{8}$$

$$F_{TPy} = -\frac{180F_s}{\pi}\sum_{i=1}^{360}\left[a_i\int_{(i-1)\pi/180}^{i\pi/180}\left\{1-\frac{\beta}{H}\left(C_r-\varepsilon\cos(\theta-\varphi)\right)\right\}\cos\varphi d\varphi\right] \tag{9}$$

Equations (8) and (9) are based on the coordinate system at rest. By rewriting eqs. (8) and (9) for the rotating reference frame, eqs. (10) and (11) are obtained,

$$F_{TPx} = -\frac{180 F_s}{\pi} \sum_{i=1}^{360} \left[a_i \int_{(i-1)\pi/180}^{i\pi/180} \left\{ 1 - \frac{\beta}{H} \left(C_r - \varepsilon \cos(\theta - \varphi) \right) \right\} \sin(\varphi - \theta) d(\varphi - \theta) \right] \tag{10}$$

$$F_{TPy} = -\frac{180 F_s}{\pi} \sum_{i=1}^{360} \left[a_i \int_{(i-1)\pi/180}^{i\pi/180} \left\{ 1 - \frac{\beta}{H} \left(C_r - \varepsilon \cos(\theta - \varphi) \right) \right\} \cos(\varphi - \theta) d(\varphi - \theta) \right] \tag{11}$$

where,

$$F_s = \frac{F}{\sum_{i=1}^{360} a_i} \qquad a_i = \begin{cases} 1 & \text{(admitted area)} \\ 0 & \text{(non-admitted area)} \end{cases}$$

The excitation forces (F_{Tx} and F_{Ty}) are assumed to be the forces deviating from the neutral position. The total excitation force F_p is decomposed to the radial and the tangential directions (F_n and F_t). The direct and cross-coupled stiffness coefficients (K_{xx} and K_{xy}) are the radial and the tangential excitation forces (F_n and F_t) divided by the amplitude of the whirling motion. These numerical treatments are expressed as follows:

$$F_{Tx} = F_{TPx}\big|_{\varepsilon=\varepsilon} - F_{TPx}\big|_{\varepsilon=0} \qquad F_{Ty} = F_{TPy}\big|_{\varepsilon=\varepsilon} - F_{TPy}\big|_{\varepsilon=0}$$

$$F_p = \sqrt{F_{Tx}^{\ 2} + F_{Ty}^{\ 2}} \qquad \psi = \tan^{-1} \frac{F_{Ty}}{F_{Tx}}$$

$$F_n = F_p \sin\left(\frac{\pi}{2} - \psi \right) \qquad F_t = F_p \cos\left(\frac{\pi}{2} - \psi \right)$$

$$K_{xx} = \frac{F_n}{\varepsilon} \qquad K_{xy} = \frac{F_t}{\varepsilon}$$

where, the treatments are based on a rotating frame of reference, and ψ is defined by Fig. 4.

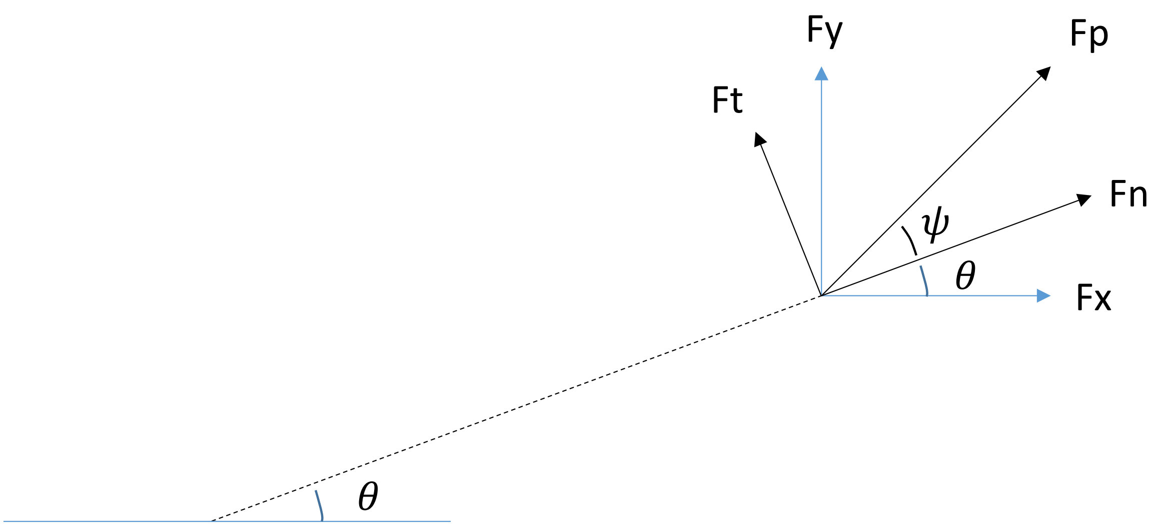

Figure 4. Definition of ψ.

C. Validation of the theoretical model

In this section, the theoretical model is validated for two cases. One is the full admission turbine dealt with by Motoi et al.[3], and the other is the partial admission steam turbine of Kanki et al.[5].

1) Validation for the full admission turbine

The LE-7A rocket turbine shaft power is 28800 kW. By using this datum, the Thomas/Alford force is estimated by this theoretical model. In this case, the Thomas coefficient β is referred as 0.56 from the paper of Motoi et al.[3]. The theoretical result of K_{xy} is 8.3×10^5 N/m by the theoretical model. Concerning unspecified data, deviation of the Thomas/Alford force between the theoretical result and the paper of Motoi et al.[3] is less than 2%. Therefore, the theoretical model is in good agreement with the paper of Motoi et al.[3].

2) Validation for the partial admission turbine

Specification of the steam turbine is listed in Table 1. Because of the lack of the data, the Thomas coefficient is an unknown parameter. As Urlichs' measured data[9] of β is about 4.5 to 5.0., β is assumed to be 5.0 in this section. The blade force is also an unknown parameter. In this case, the coefficient for the blade force is adjusted so as to be suitable for the paper of Kanki et al.[5] at one condition, and the coefficient is fixed for other conditions. By using these values and the data of Table 1, the Thomas/Alford force of the partial admission turbine is estimated by the current theoretical model. The results are shown in Fig. 5. The theoretical model can duplicate that of Kanki et al.[5]. It is concluded that the theoretical model is developed correctly.

Table 1. Specification of the partial admission steam turbine.

Tip seal clearance	0.8 mm
Rotor diameter	376.6 mm
Rotor speed	0.5 Hz
Height of turbine blade	11.6 mm
Thomas coefficient	5.0
Volume flow rate	0.15 m^3/s

Table 2. Specification of the Partial admission Turbine for Rocket Turbopump.

Shaft power	2050 kW
Rotor diameter	76 mm
Initial clearance	0.3 mm
Amplitude whirl	0.15 mm
Blade height	10 mm
Rotating speed	60600 rpm
Thomas coefficient	0.5

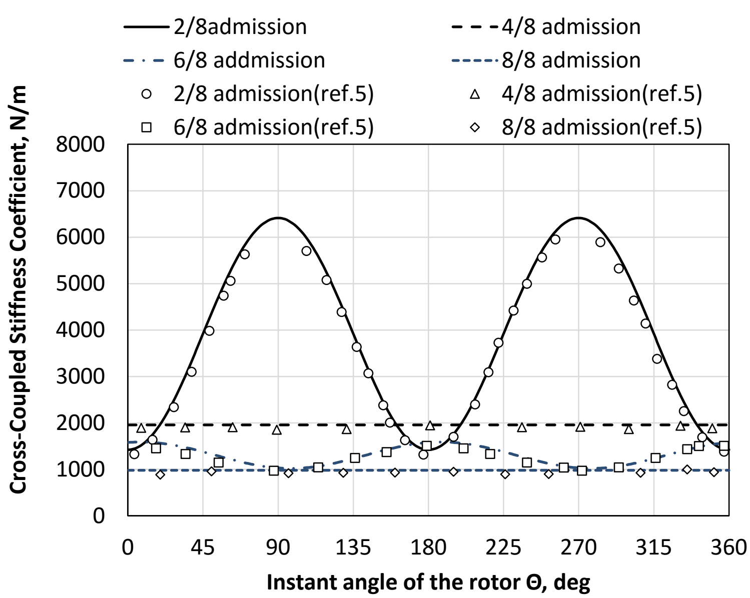

Figure 5. Cross-coupled stiffness coefficient Perturbation vs instant direction of the rotor.

III. Parametric studies of the partial admission turbine

In this section, the theoretical model is applied to some test cases at 50% partiality to find some characteristics of the partial admission turbine. The authors studied the partial admission turbine for the rocket turbopump[10]. The turbine will be discussed in following section. The specifications are listed in Table 2. To estimate the Thomas/Alford force, the Thomas coefficient is an unknown parameter. Childs' rotordynamics analysis of β is on the order of 1.0, which enables reasonable predictions for the Space Shuttle main engine (SSME) [11]. In addition, concerning the value in the paper of Motoi et al.[3], β is assumed to be 0.5 in this study. Partiality is fixed at 50%. The number of segments is changed to 1/2, 2/4, /3/6, 4/8 and 6/12 admissions as shown in Fig. 6-1 following ref.12.

1) Change the number of segments

In Fig. 6-1, the viewpoint is a cross section in the axis direction. The black area is the area of blockage, and the white area is the open area of the turbine. Calculation results are shown in Figs. 7-1 and 7-2.

As is seen from Figs. 7-1 and 7-2, the Thomas/Alford force has a constant value against the instant angle of the rotor except for 2/4 admission.

The 2/4 admission is a unique solution in that the Thomas/Alford force varies along θ. The next part is the case of the changed segment locations of the 2/4 admission.

2) Change the segment locations of the 2/4 admission

The segment locations are shown in Fig. 6-2. All of the patterns are the 2/4 admission. Calculation results are shown in Figs. 8-1 and 8-2. As is seen in Figs. 8-1 and 8-2, the Thomas/Alford force still varies against θ by changing the phase. The Thomas/Alford force in radial direction also varies along θ by changing its phase. It can be said that the segment location would not be affected by the characteristics. The number of segments would determine the characteristics. The relation of the number of segments and the Thomas/Alford force will be considered in the next section. The characteristics of the 2/4 admission are also investigated in the next section.

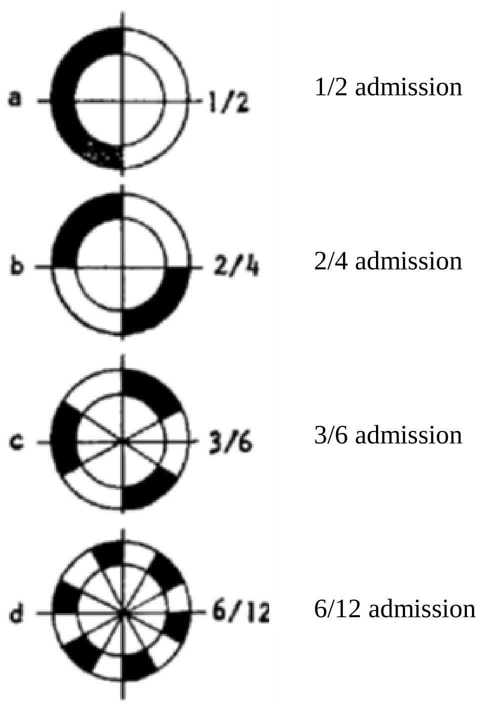

Figure 6-1. Variation of segments[12].

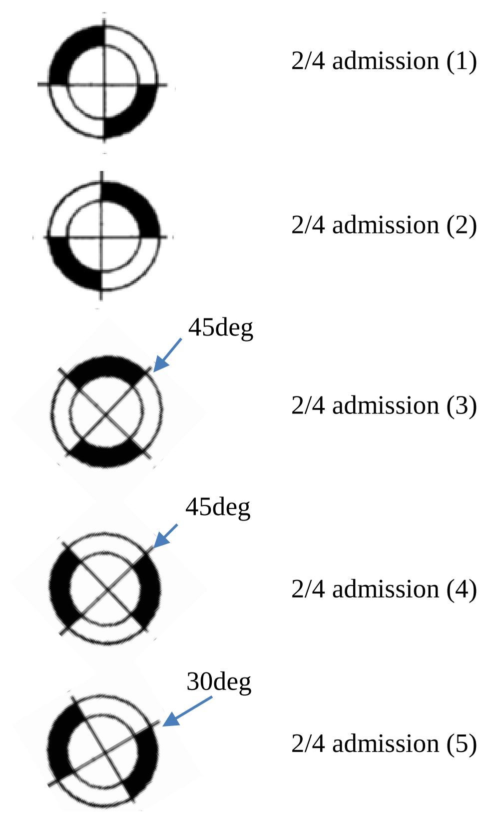

Figure 6-2. Variation of segment locations of the 2/4 admission[12].

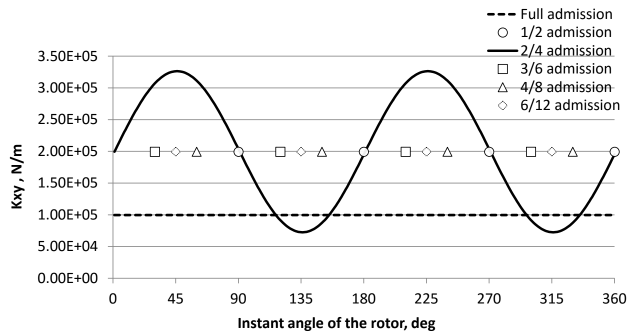

Figure 7-1. Cross-coupled stiffness coefficient with various numbers of segments.

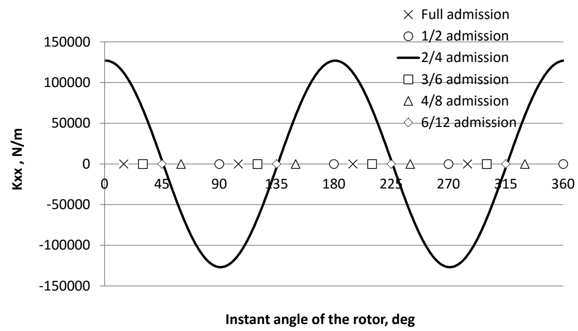

Figure 7-2. Direct stiffness coefficient with various numbers of segments.

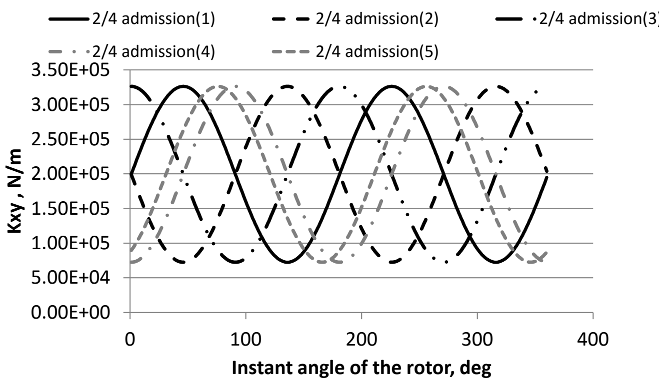

Figure 8-1. Cross-coupled stiffness coefficient of the 2/4 admission.

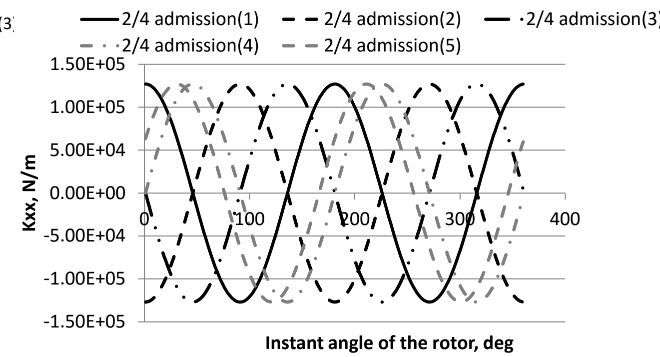

Figure 8-2. Direct stiffness coefficient of the 2/4 admission.

IV. Discussion

In the above section, the 2/4 admission is a unique solution in which the Thomas/Alford force changes against the instant angle of the rotor. The reason for this phenomenon is investigated in this section.

A. Modeling of Thomas/Alford force

As is seen from eqs. (5) and (6), the Thomas/Alford force has a 2φ trigonometric function. To extract a destabilizing force, simple trigonometric functions with the fluctuating component of the Thomas/Alford force can be defined by eqs. (12) and (13),

$$g_t \equiv \sin(2\theta - 2\varphi) \tag{12}$$

$$g_n \equiv \cos(2\theta - 2\varphi) \tag{13}$$

where, g_t is a simple function for K_{xy}, and g_n is that for K_{xx}.

B. Calculation of Thomas/Alford force model by hand

A simple model of the Thomas/Alford force as in section IV-A. is investigated as to whether the fluctuation mentioned in section III is duplicated by eqs. (12) and (13). For simplicity, 1/2, 2/4, 3/6, 4/8 and 6/12 admission are selected. Here, φ_1 is an arbitrary value between 0 and 2π.

1) 1/2 admission

$$g_t = [\sin(2\theta - 2\varphi)]_{\varphi 1}^{\varphi 2}$$
$$= \sin(2\theta - 2\varphi_1 - 2\pi) - \sin(2\theta - 2\varphi_1) = 0$$

Similarly, $g_n = 0$

2) 2/4 admission

$$g_t = [\sin(2\theta - 2\varphi)]_{\varphi 1}^{\varphi 2} + [\sin(2\theta - 2\varphi)]_{\varphi 3}^{\varphi 4}$$
$$= 2\sin(2\theta - 2\varphi_1 - \pi) - 2\sin(2\theta - 2\varphi_1) = -4\sin(2\theta - 2\varphi_1)$$

Similarly, $g_n = -4\cos(2\theta - 2\varphi_1)$

3) 3/6 admission

$$g_t = [\sin(2\theta - 2\varphi)]_{\varphi 1}^{\varphi 2} + [\sin(2\theta - 2\varphi)]_{\varphi 3}^{\varphi 4} + [\sin(2\theta - 2\varphi)]_{\varphi 5}^{\varphi 6}$$
$$= \sin\left(2\theta - 2\varphi_1 - \frac{2\pi}{3}\right) - \sin(2\theta - 2\varphi_1) + \sin(2\theta - 2\varphi_1 - 2\pi)$$
$$- \sin\left(2\theta - 2\varphi_1 - \frac{4\pi}{3}\right) + \sin\left(2\theta - 2\varphi_1 - \frac{10\pi}{3}\right) - \sin\left(2\theta - 2\varphi_1 - \frac{8\pi}{3}\right) = 0$$

Similarly, $g_n = 0$

4) 4/8 admission

$$g_t = [\sin(2\theta - 2\varphi)]_{\varphi 1}^{\varphi 2} + [\sin(2\theta - 2\varphi)]_{\varphi 3}^{\varphi 4} + [\sin(2\theta - 2\varphi)]_{\varphi 5}^{\varphi 6} + [\sin(2\theta - 2\varphi)]_{\varphi 7}^{\varphi 8}$$
$$= \sin\left(2\theta - 2\varphi_1 - \frac{2\pi}{4}\right) - \sin(2\theta - 2\varphi_1) + \sin\left(2\theta - 2\varphi_1 - \frac{6\pi}{4}\right) - \sin\left(2\theta - 2\varphi_1 - \frac{4\pi}{4}\right)$$
$$+ \sin\left(2\theta - 2\varphi_1 - \frac{10\pi}{4}\right) - \sin(2\theta - 2\varphi_1 - 2\pi) + \sin\left(2\theta - 2\varphi_1 - \frac{14\pi}{4}\right)$$
$$- \sin\left(2\theta - 2\varphi_1 - \frac{12\pi}{4}\right) = 0$$

Similarly, $g_n = 0$

5) 6/12 admission

$$g_t = [\sin(2\theta - 2\varphi)]_{\varphi 1}^{\varphi 2} + [\sin(2\theta - 2\varphi)]_{\varphi 3}^{\varphi 4} + [\sin(2\theta - 2\varphi)]_{\varphi 5}^{\varphi 6} + [\sin(2\theta - 2\varphi)]_{\varphi 7}^{\varphi 8}$$
$$+ [\sin(2\theta - 2\varphi)]_{\varphi 9}^{\varphi 10} + [\sin(2\theta - 2\varphi)]_{\varphi 11}^{\varphi 12}$$
$$= -4\sin(2\theta - 2\varphi_1) - 4\sin\left(2\theta - 2\varphi_1 - \frac{2\pi}{3}\right) + 4\sin\left(2\theta - 2\varphi_1 - \frac{\pi}{3}\right) = 0$$

Similarly, $g_n = 0$

The simple functions of eqs. (12) and (13) can duplicate in section III, and they can express the fluctuation components of the Thomas/Alford force. As a result, the 2/4 admission might be a unique solution of the Thomas/Alford force at 50% partiality.

C. Proof of the general expression

The general expression of the simple Thomas/Alford force is modeled. Proof that the 2/4 admission is a unique solution for 50% partiality is investigated.

The general expression of the simple Thomas/Alford force is shown in eqs. (14) and (15) with k/*l* admission (k, *l* is natural number and *l* = 2k).

$$g_t = \sum_{n=1}^{k} \left\{ \sin\left(2\theta - 2\varphi_1 - \frac{4}{l}(2n-1)\pi \right) - \sin\left(2\theta - 2\varphi_1 - \frac{4}{l}(2n-2)\pi \right) \right\} \tag{14}$$

$$g_n = \sum_{n=1}^{k} \left\{ \cos\left(2\theta - 2\varphi_1 - \frac{4}{l}(2n-1)\pi \right) - \cos\left(2\theta - 2\varphi_1 - \frac{4}{l}(2n-2)\pi \right) \right\} \tag{15}$$

Proof of the fact is shown in Appendix.

D. Summary

The Thomas force in the theory has a 2φ trigonometric function. The simple Thomas/Alford force model is defined by the simple trigonometric functions. The simple model indicates that the 2/4 admission is a unique solution in which the Thomas/Alford force is fluctuating with instant angle of the rotor at 50% partiality. The 2/4 admission is a contrastive case because the admission pattern and the characteristics of the Thomas/Alford force are synchronized by 2φ periodic phase from a mathematical point of view. For stable operation, the 3/6 admission is preferable because the 1/2 admission case has asymmetric blade force, and the increase in the number of segments results in an increase of partial admission loss[7,13-14] around the segments.

V. Conclusion

A theoretical model of the Thomas/Alford force of the partial admission turbine was developed and the results are listed below.

1) The theoretical model can describe the Thomas/Alford force correctly for both the full admission turbine and the partial admission turbine.
2) From parametric studies, the 2/4 admission was shown to be a unique solution which the Thomas/Alford force varies with instant angle of the rotor.
3) The reason why the 2/4 admission is a unique is that characteristics of the Thomas/Alford force are synchronized with the characteristics of the admission pattern.
4) These findings were confirmed mathematically.
5) The 3/6 admission is an adequate solution for the partial admission turbine in the case of 50% partiality.

Appendix

A. Strategy of proof for the investigation of section IV

From eq. (14), (15), $-\frac{4}{l}(2n-1)\pi$ is defined by #1, and $-\frac{4}{l}(2n-2)\pi$ is defined by #2. From the investigation of section IV-B., the patterns are categorized as follows:

[1] g_t and g_n are nonzero
Case A: terms #1 and #2 are amplified.
[2] g_t and g_n are zero
Case B: terms #1 and #2 are canceled.
Case C: each term #1 is canceled, or each term #2 is canceled.
Case D: terms #1 and #2 are complicatedly canceled.

Flow chart of the proof is shown in Fig. A.1.

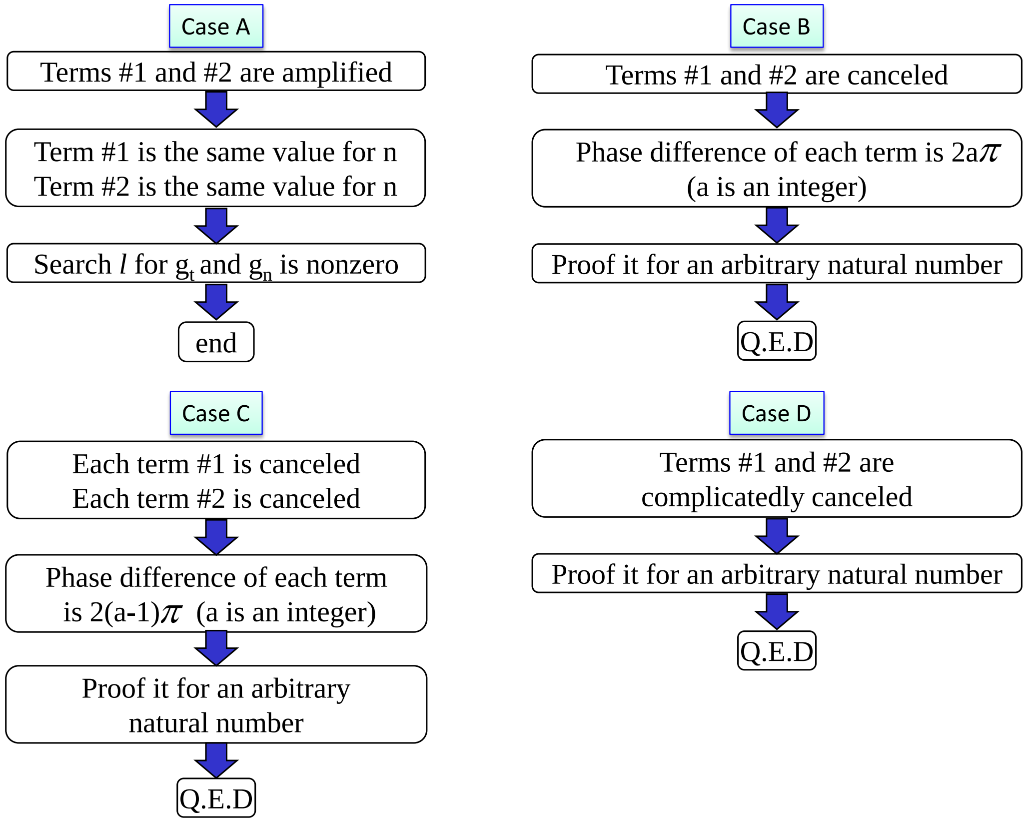

Figure A.1. Flow chart of the proof

B. Proof for the investigation of section IV

[1] g_t and g_n are nonzero

■Case A

Proof of Case A is divided into two parts, that for eq. (14) and that for eq. (15). The first pattern is a) and b), and the last pattern is c) and d).

a) Term #1 is the same value for the natural number n.
b) Term #2 is the same value for the natural number n.

If a) and b) are satisfied, g_t and g_n are nonzero (term #1 and #2 are amplified). The relationship are expressed as follows:

a) $-\frac{4}{l}(2n-1)=2n-1$

b) $-\frac{4}{l}(2n-2)=2n-2$

Since l is a natural number, only l=4 satisfies the above equations simultaneously.
On the other hand, c) and d) patterns are also possible.

c) Term #1 is the same value as term #2 for the natural number n.
d) Term #2 is the same value as term #1 for the natural number n.

Relationships c) and d) are expressed by the following:

c) $-\frac{4}{l}(2n-1)=2n-2$

d) $-\frac{4}{l}(2n-2)=2n-1$

A solution of the above equations does not exist. Therefore, g_t and g_n are nonzero by l=4. This means that 2/4 admission is a solution for which the Thomas/Alford force has changed against the instant angle of the rotor.

[2] g_t and g_n are zero

In this case, two ways are firstly considered. One way, Case B, is that the phase difference between term #1 and term #2 is $2a\pi$. The other way, Case C, is that the phase difference of each term #1 is $2(a-1)\pi$, and the phase difference of each term #2 is $2(a-1)\pi$, where a is an integer. If Case C is considered, l is a multiple number of four since the number of each term should be even. Therefore, l is divided into multiple numbers of four based on the following contents.

■Case B:

The mathematical expression of Case B is as follows, where n_1 and n_2 are natural numbers less than k.

$$2n_1-1=2n_2-2+\frac{2l}{4}a \tag{A.1}$$

l=2, l=4 is indicated before, then l=6, 10, 14, …, 4m+2, and l=8, 12, 16, ..., 4m+4 patterns are considered.

a) l=4m+2

If a=1, eq. (A.2) is derived from eq. (A.1).

$$n_1=n_2+m \tag{A.2}$$

If a=2, eq. (A.1) is as follows, and n_1 and n_2 satisfying eq. (A.1) do not exist.

$$n_1=n_2+2m+\frac{1}{2}$$

If a=3, eq. (A.1) is as follows, and n_1 and n_2 satisfying eq. (A.1) do not exist since n_1 is larger than k.

$$n_1=n_2+3m+1$$

If a is larger than 3, the case is the same as a=3. Therefore, Case B is satisfied if a=1.
In eq. (A.2), if m is larger than k, the following equation is possible by considering periodicity.

$$n_1=n_2+m-k \quad (n_2+m>k) \tag{A.2'}$$

Therefore, since m is an arbitrary natural number, g_t and g_n are zero if l=4m+2.

b) l=4m+4

If a=1, eq. (A.1) is as follows, and n_1 and n_2 satisfying eq. (A.1) do not exist.

$$n_1 = n_2 + m + \frac{1}{2}$$

If a=2, eq. (A.1) is as follows, and n_1 and n_2 satisfying eq. (A.1) do not exist.

$$n_1 = n_2 + 2m + \frac{3}{2}$$

If a=3, eq. (A.1) will be as follows, and n_1 and n_2 satisfying eq. (A.1) do not exist.

$$n_1 = n_2 + 3m + \frac{5}{2}$$

Therefore, eq. (A.1) always has a fraction, and the arbitrary natural number for l=4m+4 does not satisfy eq. (A.1). In this case, consideration of Case C is adequate.

■Case C

Since proof of the remaining pattern is l=4m+4, only l=4m+4 is considered based on the following contents. The mathematical expression of Case C is as follows:

$$2n_1 - 1 = 2n_2 - 1 + \frac{l}{4}(2a - 1)$$

From the above equation, eq. (A.3) is derived.

$$n_1 = n_2 + \frac{l}{8}(2a - 1) \tag{A.3}$$

l=4m+4 is substituted for eq. (A.3) and eq. (A.4) is derived.

$$n_1 = n_2 + \frac{1}{2}(m + 1)(2a - 1) \tag{A.4}$$

Eq. (A.4) is satisfied by m=1, 3, 5, …, 2h-1, since there is no fraction for the arbitrary natural number m. For m=2, 4, 6, 2h, m satisfying eq. (A.4) does not exit, where, h is a natural number. Case D should be introduced for m=2, 4, 6, …, 2h.

■Case D

Firstly, for l=4m+4, m=2, 4 (h=1, 2) is calculated. Next, proof of l=4m+4, m=2h for the general case is performed.

(i) h=1

If h=1 (m=2), the case is for the 6/12 admission. In this case, g_t and g_n are derived as follows:

$$g_t = -4\sin(2\theta - 2\varphi_1) - 4\left\{\sin(2\theta - 2\varphi_1)\cos\left(-\frac{2}{3}\pi\right) + \cos(2\theta - 2\varphi_1)\sin\left(-\frac{2\pi}{3}\right)\right\}$$
$$+4\left\{\sin(2\theta - 2\varphi_1)\cos\left(-\frac{\pi}{3}\right) + \cos(2\theta - 2\varphi_1)\sin\left(-\frac{\pi}{3}\right)\right\}$$
$$= -4\sin(2\theta - 2\varphi_1) + 4\left[\sin(2\theta - 2\varphi_1)\left\{-\cos\left(-\frac{2}{3}\pi\right) + \cos\left(-\frac{\pi}{3}\right)\right\}\right]$$
$$+4\left[\cos(2\theta - 2\varphi_1)\left\{-\sin\left(-\frac{2}{3}\pi\right) + \sin\left(-\frac{\pi}{3}\right)\right\}\right]$$
$$= -4\sin(2\theta - 2\varphi_1) + 4\sin(2\theta - 2\varphi_1)\left\{-\cos\left(-\frac{2}{3}\pi\right) + \cos\left(-\frac{\pi}{3}\right)\right\}$$
$$= -4\sin(2\theta - 2\varphi_1) - +4\sin(2\theta - 2\varphi_1)\left\{\cos\left(\pi - \frac{2}{3}\pi\right) + \cos\left(-\frac{\pi}{3}\right)\right\}$$
$$= -4\sin(2\theta - 2\varphi_1) + 4\sin(2\theta - 2\varphi_1)\left\{2\cos\left(\frac{\pi}{3}\right)\right\}$$

$$g_n = -4\cos(2\theta - 2\varphi_1) + 4\cos(2\theta - 2\varphi_1)\left\{2\cos\left(\frac{\pi}{3}\right)\right\}$$

Therefore, g_t and g_n are zero by periodicity.

(ii) h=2

If h=2 (m=4), g_t and g_n will be the following expressions.

$$g_t = -4\cos(2\theta - 2\varphi_1) + 4\cos(2\theta - 2\varphi_1)2\left\{\cos\left(\frac{\pi}{5}\right) - \cos\left(\frac{2}{5}\pi\right)\right\}$$
$$g_n = -4\sin(2\theta - 2\varphi_1) + 4\sin(2\theta - 2\varphi_1)2\left\{\cos\left(\frac{\pi}{5}\right) - \cos\left(\frac{2}{5}\pi\right)\right\}$$

From $\cos\frac{\pi}{5} = \frac{1+\sqrt{5}}{4}$, $\cos\frac{2}{5}\pi = \frac{\sqrt{5}-1}{4}$, g_t and g_n are zero.

(iii) m=2h

In general, g_t and g_n are derived by the following for m=2, 4, 6, …, 2h

$$g_t = -4\sin(2\theta - 2\varphi_1) + 4\sin(2\theta - 2\varphi_1)2\sum_{j=1}^{h}\left\{\cos\left(\frac{2j-1}{2h+1}\pi\right) - \cos\left(\frac{2j}{2h+1}\pi\right)\right\} \quad \text{(A.5)}$$

$$g_n = -4\cos(2\theta - 2\varphi_1) + 4\cos(2\theta - 2\varphi_1)2\sum_{j=1}^{h}\left\{\cos\left(\frac{2j-1}{2h+1}\pi\right) - \cos\left(\frac{2j}{2h+1}\pi\right)\right\} \quad \text{(A.6)}$$

In eq. (A.5) and (A.6), if $\sum_{j=1}^{h}\left\{\cos\left(\frac{2j-1}{2h+1}\pi\right) - \cos\left(\frac{2j}{2h+1}\pi\right)\right\}$ of RHS is satisfied with eq. (A.7), g_t and g_n will be zero.

$$\sum_{j=1}^{h}(-1)^{j+1}\cos\left\{\frac{j\pi}{2h+1}\right\} = \frac{1}{2} \quad \text{(A.7)}$$

Eq. (A.7) of LHS is expanded to eq. (A.8) [15].

$$\frac{1}{2}\left[-\cos\left\{\frac{\pi}{2}(1+2h)\right\}\sec\left\{\frac{\pi}{2(1+2h)}\right\} - \cos\left\{\frac{\pi}{2}\frac{(1+4h)}{(1+2h)}\right\}\sec\left\{\frac{\pi}{2(1+2h)}\right\}\right] \quad \text{(A.8)}$$

First term of eq. (A.8), $\cos\left\{\frac{\pi}{2}(1+2h)\right\}$, is odd times of $\cos\frac{\pi}{2}$, and thus it will be zero. The second term of eq. (A.8) is as follows.

$$-\cos\left\{\frac{\pi}{2}\frac{(1+4h)}{(1+2h)}\right\}\sec\left\{\frac{\pi}{2(1+2h)}\right\} = -\cos\left\{\frac{2+4h}{2(1+2h)}\pi - \frac{\pi}{2(1+2h)}\right\}\sec\left\{\frac{\pi}{2(1+2h)}\right\}$$

$$= -\cos\left\{\pi - \frac{\pi}{2(1+2h)}\right\}\sec\left\{\frac{\pi}{2(1+2h)}\right\} = \cos\left\{\frac{\pi}{2(1+2h)}\right\}\sec\left\{\frac{\pi}{2(1+2h)}\right\} = 1$$

Therefore, eq. (A.7) is satisfied for an arbitrary natural number h. Then, g_t and g_n are zero for l=4m+4, m=2, 4, 6, …, 2h.

From the results of Case A through Case D, the 2/4 admission is a unique solution for which the Thomas/Alford force has changed against the instant angle of the rotor. (Q.E.D)

Acknowledgments

The authors are grateful to Professor Tsuyoshi Inoue of Nagoya University for useful discussion. The authors would also like to thank Hiromichi Hiraki of JAXA and Dr. Yoshiki Yoshida for useful advice.

References

[1]Thomas, H. J., “Instabile Eigenschwingungen von Turbinenlaeufern, Angefacht durch die Spaltstroemung in Stopfbuchsen und Beschauflung,” Bull. de l’A.I.M., 71, No.11/12, 1958, pp. 1039-1063.

[2]Alford, J. S., “Protecting Turbomachinery From Self-Excited Rotor Whirl,” ASME Journal of Engineering for Power, Oct. 1965, pp. 333-343.

[3]Motoi, H., Kitamura, A., Sakazume,N., Uchiumi, M., Uchida, M., Sakaki, K., Nozaki, O. and Iwatubo, T., “Sub-Synchronous Whirl In The LE-7A Rocket Engine Fuel Turbo-Pump,” ISCORMA-2, Poland, Aug. 2003, pp. 1-10.

[4]Hendricks, R. C., Tam, L. T. and Muszynska. A., “Turbomachine Sealing and Secondary Flows, Part2 – Review of Rotordynamics Issues in Inherently Unsteady Flow Systems With Small Clearances,” NASA TM-2004-211991, 2004.

[5]Kanki, H. and Tanitsuji, A., “Stability of High Pressure Turbine Under Partial Admission Condition,” ASME IDETC/CIE 2005, Sep. 2005, DETC2005-84774.

[6]Maurice, L. A., *Rotating Machinery Vibration, from Analysis to Troubleshooting,* Marcel Dekker, Inc., 2001.

[7]Horlock, J. H., *Axial flow Turbines*, Butterworths, 1966.

[8]Linhardt, H. D. and Silvern, D. H.., “Analysis of Partial Admission Axial Impulse Turbines,” American Rocket Society Journal, 1961, pp. 297-308.

[9]Urlichs, K., “Clearance Flow Generated Transverse Forces at the Rotors of Thermal Turbomachines,” NASA TM-77292, 1975.

[10]Yada, K., Shimiya, N., Uchiumi, M., Tokuyama, Y. and Funazaki, K., “Optimized Aerodynamic Design of the Turbine for a Rocket Trubopump,” AJCPP2016, Takamatsu, JAPAN, Mar. 2016, AJCPP2016-008.

[11]Childs, D., *Turbomachinery Rotordynamics, Phenomena, Modeling & Analysis*, John Wiley & Sons, Inc., 1993.

[12]“Liquid Rocket Engine Turbines,” NASA SP-8110, 1974.

[13]Frolov, V. V., and Ignatevskh, E. A., “Edge Losses of Energy in Partial Admission Turbine Stages,” Teploenergetika, Vol. 18, No. 1, 1971, pp.77-79.

[14]Frolov, V. V., and Ignatevskh, E. A., “Calculating the Windage Losses in a Turbine Stage,” Teploenergetika, Vol. 19, No. 11, 1972, pp.33-37.

[15]*Mathmatica10.1 User Gide*, Wolfram Research, Inc., 2015.